Am J Transl Res 2024;16(7):2898-2909
www.ajtr.org /ISSN:1943-8141/AJTR0156827

Original Article

Case report and functional verification of a novel mutation in the interferon regulatory transcription factor 6 gene in a family with orofacial clefts

Fengjuan Ding, Fei Hou, Shan Shan, Yan Zhao, Hua Jin

Department of Prenatal Diagnosis Center, Jinan Maternal and Child Health Hospital, Jinan 250001, Shandong, China

Received March 27, 2024; Accepted May 29, 2024; Epub July 15, 2024; Published July 30, 2024

Abstract: Background: This study aimed to identify the causative genetic variant in a Chinese family with orofacial clefts. Methods: We retrospectively analyzed the clinical information of a family with orofacial clefts. Then, we performed an etiological genetic analysis of the family using whole exome sequencing analysis and Sanger sequencing. We created a hybrid code-shifting mutation cell line (293T-462het) and evaluated its impact on cell proliferation, migration, and apoptosis, as well as E-cadherin and vimentin expression. Results: Whole exome sequencing revealed a novel heterozygous variant c.1386del (p.A462Pfs*28) in the interferon regulatory transcription factor 6 (*IRF6*) gene in a family with orofacial clefts. Sanger sequencing further confirmed that this heterozygous variant was the genetic cause of orofacial clefts in this family. The c.1386del variant of *IRF6* was classified as likely pathogenic. The heterozygous mutation *IRF6* (c.1386del) enhanced cell proliferation and migration while inhibiting cell apoptosis and regulating the expression of E-cadherin and vimentin. Conclusion: This study identified a novel c.1386del mutation in the *IRF6* gene and explored how this mutation leads to lip and palate defects. Our results provide a solid theoretical foundation for future genetic detection of these orofacial defects.

Keywords: Orofacial cleft, *IRF6*, next-generation sequencing, prenatal diagnosis, functional verification

Introduction

Orofacial clefts are among the most prevalent structural birth defects. The malformations during craniofacial development prevent proper tissue fusion of the upper lip, palate, or both [1]. The incidence of orofacial clefts varies according to geographic factors, ethnicity, and socioeconomic status, and the global prevalence is approximately 1.244% [2]. In China, the prevalence of cleft lip and palate is slightly higher (approximately 1.4%) [3]. Recent years have seen an increase in the incidence of cleft lip and palate across various countries. The most common types of orofacial clefts are cleft lip with or without cleft palate and isolated cleft palate. Non-syndromic orofacial clefts account for 70% of patients with cleft lip with or without cleft palate, and 50% of those with isolated cleft palate. The pathogenic mechanisms of non-syndromic orofacial clefts are complex, involving both genetic and environmental factors and their interactions. However, the specific mechanisms have not been fully elucidated.

Ultrasonography is the routine imaging method to detect orofacial clefts. However, due to the relatively small facial area of the fetus in the first trimester of pregnancy, ultrasound examination is challenging. With advances in ultrasonography and magnetic resonance imaging (MRI) technologies, the detection rates of orofacial cleft in the second trimester are gradually increasing, but missed diagnoses still occur. Children born with orofacial clefts experience significant feeding difficulties, speech impairments, recurrent middle ear infections, and dental defects [4]. Surgery is the mainstay of treatment for facial malformations. Long-term multidisciplinary management of orofacial clefts can pose substantial medical, psychological, social, and economic burdens for patients and their families [5]. Therefore, elucidating the pathogenesis of orofacial clefts is necessary to

https://doi.org/10.62347/IAQV2788

improve our understanding of the disease and facilitate appropriate genetic counseling.

Advances in next-generation sequencing technologies have enabled the identification of genetic causes of orofacial clefts and established diagnosis at the molecular level. This information provides the basis for future genetic counseling and prenatal diagnosis, allowing families to make informed decisions. Based on clinical assessment, we performed a whole exome sequencing (WES) analysis on a lineage of individuals with a history of cleft lip and palate, including a couple with multiple children with cleft lip and palate. Site verification was conducted simultaneously. We identified a heterozygous frameshift mutation (p.A462Pfs*28) in the interferon regulatory transcription factor 6 (*IRF6*) gene as the likely causative defect in this family. Identification of this variant has not been previously reported and thereby expands the mutational spectrum of cleft lip and palate. We also investigated the influence of this novel *IRF6* site mutation on cell proliferation, apoptosis, and epithelial-mesenchymal cell transformation (EMT) to explore the mechanism(s) through which this mutation leads to orofacial clefts. Our findings offer a theoretical basis for future genetic detection of cleft lip and palate.

Methods and materials

Subjects and clinical information

The family with cleft lip and palate described in this paper was from Jinan City, Shandong Province, China. Clinical information and peripheral blood samples were obtained from the recruited family members. Written informed consent was obtained from all participating family members, and the study was approved by the Medical Ethics Committee of Jinan Maternal and Child Health Hospital (2021-1-047).

Whole exome sequencing

The proband and his wife each provided 2 mL of peripheral blood for analysis. Fetal samples (IV7) were collected from amniotic fluid during invasive prenatal diagnosis. DNA was extracted using a standard phenol-chloroform protocol. WES was performed in the proband and his wife using the Illumina NovaSeq 6000 system, with an average sequencing depth of 200X, as previously described [6]. Following bioinformatics analysis, the variant's pathogenicity was evaluated according to the American Academy of Medical Genetics and Genomics (ACMG) guidelines [7].

Knock-out plasmid design and construction

Deletion of thymine (T) (c.1386del) at position 1386 of the target gene IRF6 resulted in a frameshift mutation and substitution of proline (p.A462P) for alanine at position 462 of the protein amino acid sequence. The pXC9-IRF6-A462P-knock-out (KO) plasmid was designed and synthesized as follows: 1) BsmBI was used to digest the pXC9 plasmid to obtain a vector fragment; 2) three pairs of small guide RNAs (sgRNA) targeting the mutation site were designed, namely sgRNA-1 (forward: ACCCCA GACATCAAGGATAA; reverse: TTATCCTTGATGTC-TGGGGT), sgRNA-2 (forward: TCCTTCAAACCC-AGGAGAGC; reverse: GCTCTCCTGGGTTTGAAG-GA), and sgRNA-3 (forward: TACTGGGGAGGC-AGGGCAGG; reverse: CCTGCCCTGCCTCCCCAG-TA); 3) denaturation and annealing processes were performed to obtain sgRNA double-stranded DNA fragments; 4) T4 DNA ligase was used to connect the three pairs of fragments; and 5) the constructed plasmid was transformed and subsequently extracted for sequence analysis.

Donor plasmid design and construction

The homologous recombinant pUC19-donor plasmid was designed and synthesized to target the predicted sgRNA KO site; the expected KO target fragment was 224 bp in length. To more efficiently clone the A462P mutant fragment into the cell genome, 200-bp upstream and downstream homology arm sequences were added to the two sides of the A462P mutant fragment. A segment of sgRNA was added on both sides of the upstream and downstream homology arms to enhance expression efficiency of the homologous recombinant sequence. The final fragment (676 bp in length) was synthesized by Anhui General Biological Co. Ltd.; the pUC19 plasmid was digested with EcoRI and KpnI; and the homologous recombinant sequence was then ligated with T4 DNA ligase, transformed, digested, and sequenced.

Construction of mutant cell lines

HEK-293T cells were purchased from the Shanghai Institute of Cell Biology of the Chinese

Academy of Sciences (Shanghai, China). For construction of heterozygous frameshift mutant cell lines, 1 × 10^6 cells in the log phase were inoculated into 6-well plates, after which 2 mL of Dulbecco's Modified Eagle Medium (DMEM; Gibco, Carlsbad, CA, USA) containing 10% fetal bovine serum (FBS) Gibco was added. The cultures were grown at 37°C in an incubator supplied with 5% carbon dioxide (CO_2) (Thermo Fisher, Waltham, MA, USA). Transfection was performed when the cell confluence reached 90%. For transfection, 2 μg of pXC9-IRF6-A462P-KO plasmids (KO-1, KO-2, and KO-3) and 2 μg of pUC19-donor plasmid were added to 100 μL of Opti-MEM reduced serum medium. After thorough mixing, 8 μL of Turbofect (Thermo Fisher) was added. The mixture was left undisturbed for 20 minutes, after which DMEM with 10% FBS was added. pLVSO2 plasmid was used as a positive control and transfected after 1 h.

Next, 1 μg/mL puromycin was added to each well to screen for positive clones. After continuous 10-day screening, single clones were picked, and the DNA of single clones was amplified using polymerase chain reaction (PCR). The PCR amplification products were identified by sequencing, and positive clones were selected for expansion. The forward and reverse primer sequences for PCR amplification of A462P were TGAACAGGTCATTCCAGTAGTG and TCACAATTACTGGGGAGGC, respectively. PCR was performed as follows: denaturation at 94°C for 20 s, annealing at 60°C for 20 s, and extension at 72°C for 30 s for a total of 30 cycles. The amplified fragment was 238 bp in length.

Cell proliferation assay

After stable culture for 48 days, cell proliferation ability was assessed using the Cell Counting Kit-8 (CCK-8) assay. The cells were inoculated into a 96-well plate at 8000 cells/well and cultured for 24, 48, and 72 h. Next, 10 μL of CCK-8 solution (Shanghai Beyotime Biotechnology, Shanghai, China) was added to each well at each time point, and the culture plate was incubated for 2 h at 37°C in an incubator supplied with 5% CO_2. Absorbance at 450 nm was measured using a microplate reader (Thermo Fisher). Statistical values were calculated, and a growth curve was constructed.

Transwell migration assay

The cells were starved for 12 h in a serum-free medium in a transwell chamber placed in a 24-well plate. The cells were inoculated into the chamber at 5 × 10^4 cells/well. Next, 500 μL of complete medium was added to the lower chamber. The culture plate was incubated for 24 h at 37°C in an incubator supplied with 5% CO_2. After this, the cells were washed twice with phosphate-buffered saline (PBS) and then fixed with 4% paraformaldehyde for 20 min. Next, the cells were washed twice with PBS and stained with 0.1% crystal violet (Guangzhou Saiguo Biotech, Guangzhou, Guangdong, China) for 15 min. Non-migrating cells in the upper chamber were gently removed with a medical cotton swab. The chamber membrane was cut using a blade, placed on a glass slide, and covered with neutral resin. The stained cells were visualized and counted under a microscope.

Flow cytometry apoptosis assay

Cells were separated by trypsinization when they were approximately 70% full. The cells were collected, washed once with PBS, and then washed with 1 × Binding Buffer before being resuspended in this buffer. The number of cells in each sample was counted, 100 μL of 1 × Binding Buffer was added, and the number of cells in each tube was adjusted to 1 × 10^6. Five μL of Annexin V-allophycocyanin (V-APC; Multisciences [Lianke] Biotech, Hangzhou, Zhejiang, China) and 10 μL of 7-aminoactinomycin D (7-AAD; Multisciences [Lianke] Biotech) were added, after which the mixtures were vortexed, mixed, and stored at room temperature in the dark for 15 min. Next, 485 μL of pre-cooled 1 × Binding Buffer was added, followed by resuspension and further mixing. The samples were subsequently loaded into the flow cytometer (ACEA Biosciences, San Diego, CA, USA) for detection, and NovoExpress software was used to analyze the data.

Reverse transcription-quantitative polymerase chain reaction

Total RNA was extracted from cells using Trizol reagent (Bioteke Corporation, Beijing, China), and the concentration and purity of RNA samples were determined. RNA was reverse transcribed following the instructions provided by the manufacturer of the reverse transcription

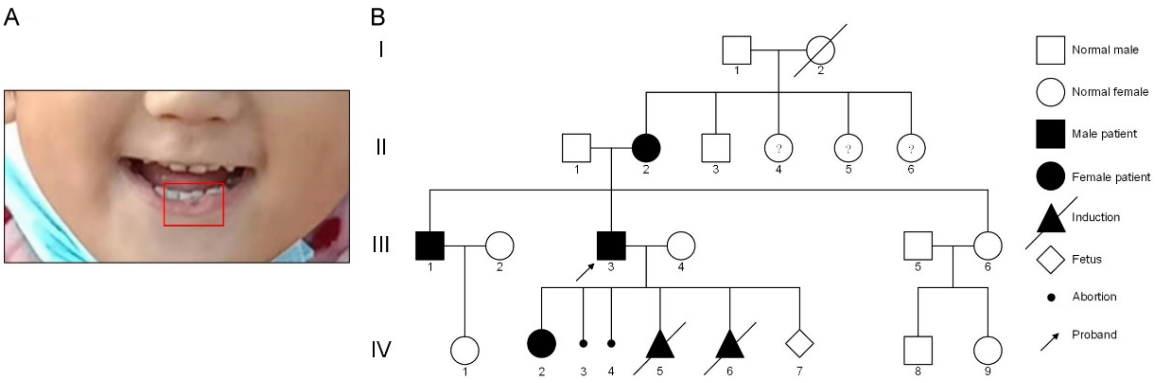

Figure 1. Photograph of the daughter (IV2) of the proband and pedigree of the interferon regulatory transcription factor 6 (*IRF6*) gene variant in the family. A: The little girl had a cleft lip and palate, and a lower lip depression can still be seen after surgical treatment (as indicated by the red box). B: Family diagram showing individuals with or without cleft lip and palate. Family members I1, II2, II3, III1, III3, III4, III6, IV2, and IV7 all underwent testing, whereas II4, II5, and II6 refused testing for personal reasons. Note: I, II, III, and IV represent the generations. Squares represent males, large circles represent females, solid black symbols indicate affected patients, the arrow indicates the proband, '?' represents family members who did not undergo gene sequencing, small circles indicate abortions, triangles indicate labor inductions, and the diamond indicates the current fetus.

(RT) kit (Thermo Fisher). The SYBR Green qPCR Detection Kit (Thermo Fisher) was used for quantitative PCR (qPCR) analysis using the synthesized cDNA template. RT-qPCR was performed as follows: pre-denaturation at 95°C for 5 min, followed by 40 cycles of denaturation at 95°C for 30 s, annealing at 60°C for 30 s, and extension at 72°C for 15 s. The PCR products were quantified using the relative quantitative 2-ΔΔCT method. The primer sequences were as follows: β-actin: forward, TGGCACCAGCACAATGAA, reverse, CTAAGTCATAGTCCGCCTAGAAGCA; IRF6, forward, GTCATTCCAGTAGTGGCTCGG, reverse, TTACTGGGGAGGCAGGGCAG; E-cadherin: forward, CGTCCTGGGCA GAGTGAATTT, reverse, GTCCCAGGCGTAGACCAAGA; and vimentin: forward, TGACCT TGAACGCAAAGTGGA, reverse, CAGAGAGGTCAGCAAACTTGGA.

Statistical methods

Data were analyzed using SPSS 22.0 software. All values were expressed as mean ± standard deviation. Pairwise comparisons were conducted using independent samples t-test, with $0.01<P<0.05$ indicating a statistically difference; $P<0.01$ indicating a significant difference; and $P<0.001$ indicating a very significant difference.

Results

Clinical features of the family

The proband (III3), aged 32 years, had an orofacial cleft. He and his 26-year-old wife (III4) had a family history of orofacial cleft. Their currently living daughter (IV2) was born with the disease (**Figure 1A**), and they previously had two unexplained embryonic discontinuations and two labor inductions because of an orofacial cleft. The proband's elder brother (III1) and mother (II2) also had an orofacial cleft. At the time of this study, the gestational age of the couple's fetus (IV7) was 13 weeks. The couple had received genetic counseling at the Prenatal Diagnosis Center of Jinan Maternity and Child Health Hospital. Amniocentesis was performed to extract amniotic fluid from the fetus for WES. The family pedigree is shown in **Figure 1B**. Physical examination revealed no abnormalities in other organ systems.

Identification of the pathogenic genetic variant

To identify the causative variant of this family, we conducted WES of the proband (III3) and his wife (III4). This bioinformatics analysis revealed a novel heterozygous variant c.1386del (p.A462Pfs*28, hg19, NM_006147) within the *IRF6* gene in the proband. This mutation was not found in control populations, including the Exome Sequencing Project (ESP), 1000 Genomes Project, and Exome Aggregation Consortium (ExAC) databases. WES of the couple's fetus (IV7) revealed no evidence of the *IRF6* mutation, and the couple chose to continue the pregnancy.

Sanger sequencing was performed to detect the *IRF6* variant among the pedigree members,

including I1, II2, II3, III1, III3, III4, III6, IV2, IV7, and IV6. This sequencing revealed that the variant was inherited from the proband's affected mother (II2). Additionally, the proband's affected older brother (III1) and his daughter (IV2) were also identified as mutant c.1386del carriers (**Figure 2**). This mutation was not found in population databases (ACMG criteria: PM2) and was identified as a frameshift mutation in the last exon. The mutation was predicted to not cause nonsense-mediated mRNA decay, but potentially change the length of the protein (PVS1-moderate). The *IRF6* mutation carriers (II2, III3, III1, and IV2) exhibited orofacial clefts that corresponded to a single genetic disorder (PP1+PP4). Following the ACMG guidelines, the c.1386del (p.A462Pfs*28) variant was classified as "likely pathogenic" (PM2+PVS1-moderate+PP1+PP4) [5]. Based on these findings, we deduced that the c.1386del (p.A462Pfs*28) *IRF6* variant was responsible for the pathogenesis of this family's orofacial clefts.

The IRF6 (c.1386del) variant promoted cell proliferation and migration and inhibited cell apoptosis

To explore the effects of the *IRF6* (c.1386del) variant on cell function, we performed CCK-8, transwell migration, and flow cytometry apoptosis assays on wild-type (293T-WT) and mutant (293T-462het) cells. The CCK-8 assay revealed that cell viability was significantly higher in 293T-462het cells than that in 293T-WT cells at 48 h ($P<0.05$) and 72 h ($P<0.01$) after transfection (**Figure 3**). In the transwell assay, the number of 293T-WT cells was 22.667±2.082, whereas the 293T-462het cells was 46.000±3.606, indicating that the *IRF6* (c.1386del) variant significantly promoted cell migration ($P<0.001$; **Figure 4**). The evaluation of cell apoptosis rates, conducted via Annexin V-APC and 7-AAD dual-stained flow cytometry, revealed a significant reduction in 293T-462het cells (4.670±0.061%) compared to 293T-WT cells (7.253±0.248%) ($P<0.01$; **Figure 5**).

Mutant IRF6 (c.1386del) regulated the expression of E-cadherin and vimentin

The effects of mutant *IRF6* (c.1386del) on expression of E-cadherin and vimentin at the mRNA level were evaluated using RT-qPCR. The results revealed that expression of both *IRF6* and E-cadherin was lower in 293T-462het cells than in 293T-WT cells, whereas expression of vimentin was significantly higher in 293T-462het cells than in 293T-WT cells (**Figure 6**).

Discussion

In the current study, we used WES data and subsequent Sanger sequencing verification to detect a heterozygous mutation c.1386del (p.A462Pfs*28) within the *IRF6* gene in a family with cleft lip and palate. The affected family members (II2, III1, III3, and IV2) exhibited varying degrees of cleft lip and palate, and each carried the heterozygous mutation c.1386del (p.A462Pfs*28). This variant was not present in databases from control populations (ESP, the 1000 Genomes Project, and ExAC) and has not been previously reported in the literature. Based on ACMG guidelines, the c.1386del variant in *IRF6* was classified as "likely pathogenic," meeting the criteria of PM2+PVS1-moderate+PP1+PP4. As this mutation has not been reported, our results expand the known mutation spectrum of *IRF6* in cleft lip and palate and provide a theoretical basis for future genetic detection of orofacial clefts.

IRF6, a member of interferon regulator family, features a highly conserved DNA-binding domain (amino acids 13-113) and a protein-binding domain (amino acids 226-394) called Smad-interferon regulatory environment (SMIR). The *IRF6* gene plays an important role in the formation of facial structures, including the lips, palate, teeth, and tongue. *IRF6*-related diseases include cleft mouth type 6, popliteal pterygium syndrome (PPS), and Van der Woude syndrome (VWS), which are autosomal dominant diseases. The clinical manifestations of PPS are mainly cleft lip and palate, abnormal development of the reproductive system, popliteal webbing, spinal fissure, clubfoot, and various skin, finger, and toe deformities [8]. PPS exhibits significant clinical heterogeneity. VWS, a typical cleft lip and palate syndrome, is an inherited developmental disorder characterized by a depression in the lower lip or sinuses, cleft lip, or cleft palate [9]. The clinical manifestations of cleft mouth type 6 predominantly include nonsyndromic cleft lip and palate [10]. In the family described in this report, the affected members (II2, III1, III3, and IV2) exhibited cleft lip and palate, with no other abnormalities detected on physical examination. In addition, the proband's wife (III4) had previously given

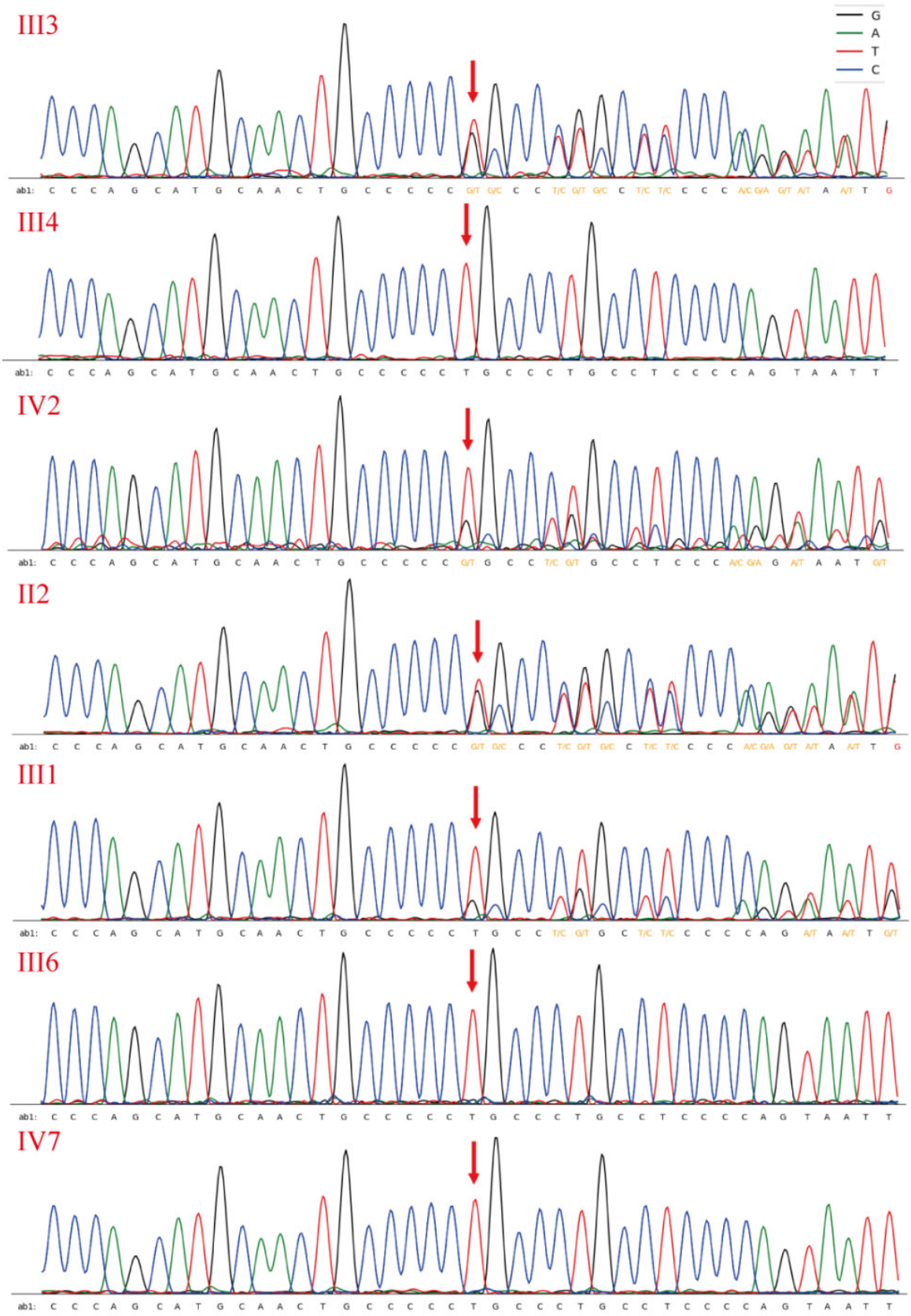
III3
G
A
T
C
III4
IV2
II2
III1
III6
IV7

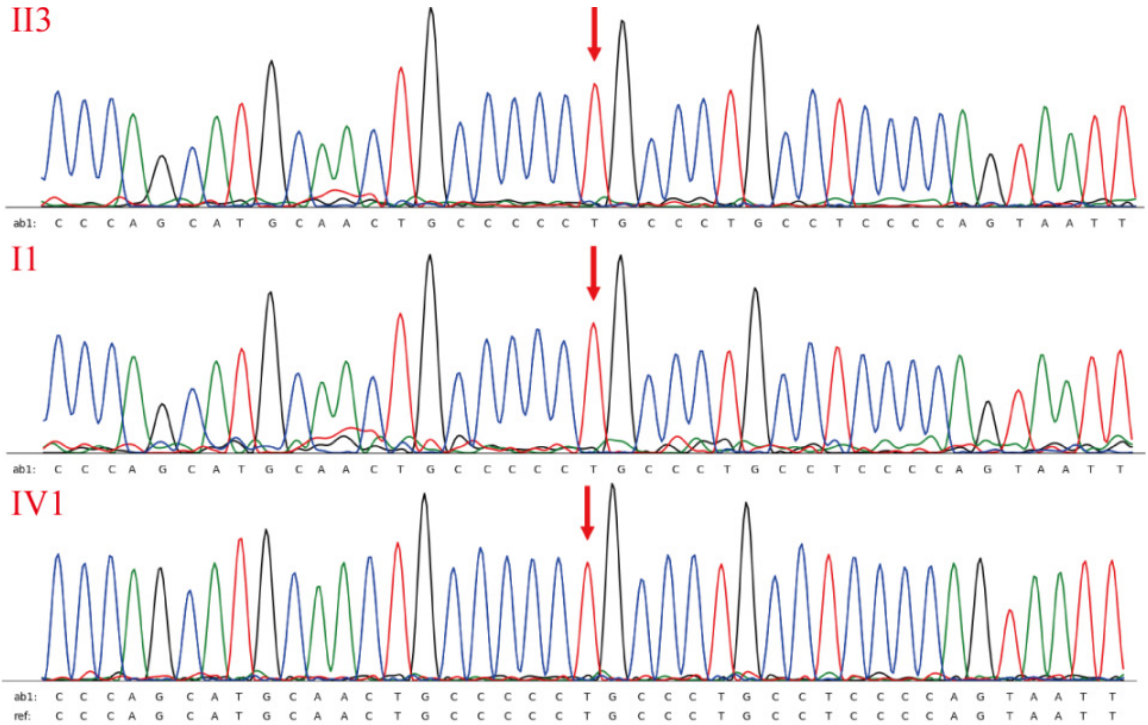

Figure 2. Verification of the interferon regulatory transcription factor 6 (*IRF6*) gene variant in the family by Sanger sequencing.

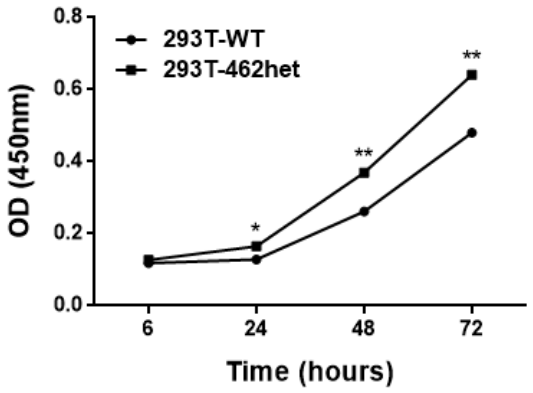

Figure 3. The heterozygous mutation c.1386del (p.A462Pfs*28) within the interferon regulatory transcription factor 6 (*IRF6*) gene promoted cell proliferation. 293T-WT represents wild-type (control) HEK-293T cells, and 293T-462het represents HEK-293T cells heterozygous for the *IFR6* mutation. *P<0.05, **P<0.01. OD, optical density.

birth to a daughter (IV2) with cleft lip and palate. The couple had four other conceptions, but these pregnancies were terminated prior to birth (embryo terminations [IV3 and IV4] and labor inductions with cleft lip and palate [IV5 and IV6]). Fortunately, their current fetus (IV6) does not carry the c.1386del (p.A462Pfs*28) mutation in *IRF6* gene. Overall, discovering this new mutation offers a valuable foundation for providing genetic counseling and conducting additional prenatal diagnoses for families at risk.

A previous study of the prevalence and distribution of *IRF6* exon mutations in 307 families with VWS syndrome and 37 families with PPS syndrome found that the distribution of mutations was not random. Most mutations were located in exons 3, 4, 7, and 9 in VWS, and exons 3, 4, and 9 were also the most common location of mutations in PPS [11]. The mutations causing VWS included stop mutations, DNA binding, missense mutations within the SMIR and DNA-binding domains, and splicing mutations, resulting in haploinsufficiency of the *IRF6* gene [11]. Most mutations causing PPS are missense mutations involving DNA-binding domains but not affecting protein-binding activity or mutations that cause a dominant negative effect at the recessive splicing site, which explains the severity of the phenotype [12]. The missense mutations causing VWS are almost evenly distributed between the DNA-binding and SMIR domains. In contrast, most missense mutations responsible for PPS are found in the

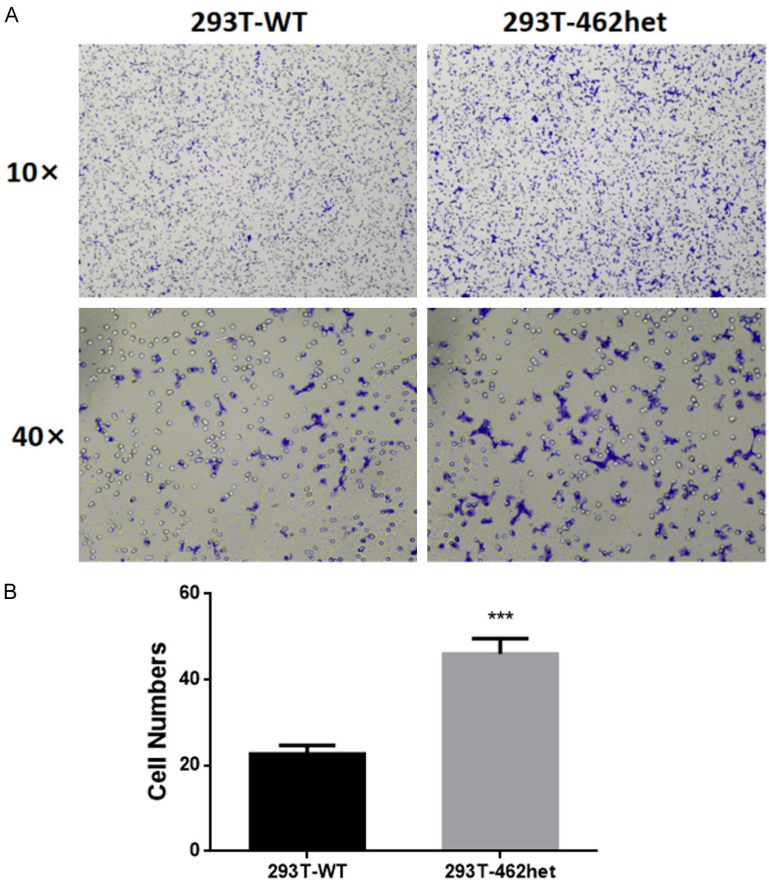

Figure 4. The heterozygous mutation c.1386del (p.A462Pfs*28) within the interferon regulatory transcription factor 6 (*IRF6*) gene promoted migration. A: Transwell experimental results. B: Comparison of the number of cell invasions in each group. 293T-WT represents wild-type (control) HEK-293T cells, and 293T-462het represents HEK-293T cells heterozygous for the *IFR6* mutation. ***P<0.001.

DNA-binding domain. These findings suggest that missense mutations in the DNA-binding domains associated with VWS and PPS have different effects on IRF6 function. A possible explanation for these genotype-phenotype relationships is that missense mutations responsible for VWS lead to total loss of function of the mutated IRF6 protein, which affects both DNA- and protein-binding, whereas missense mutations responsible for PPS only affect the ability of IRF6 to bind to DNA [13]. Few studies have reported frameshift mutations of the *IRF6* gene in *IRF6*-related genetic diseases. Interestingly, the novel c.1386del (p.A462Pfs*28) mutation in the *IRF6* gene described in this study is a frameshift mutation in the last exon (exon 9).

The pathogenesis of cleft lip and palate is a complex process involving many cellular processes, including proliferation of mesenchymal cells and epithelial cells, neural crest induction, EMT, cell migration, apoptosis, signal transduction through primary cilia, epithelial seam formation and disappearance, periderm formation and removal, and interactions with the extracellular matrix [14]. EMT is regulated by the Pbx-Snail1/Smad-E-cadherin pathway, which may interact with pre-B-cell leukemia transcription factor (Pbx)-regulated apoptosis [15]. The *IRF6* gene is necessary for craniofacial morphogenesis and ectoderm formation during embryonic development. Besides its involvement in epithelial cell proliferation and differentiation, IRF6 exhibits dynamic expression in the ectoderm, periderm, oral epithelium, and tooth germ of embryonic tissue [16]. In an *IRF6* KO mouse model, the *IRF6* defect resulted in inhibited apoptosis of mid-palate ridge epithelial cells, preventing complete fusion of mesenchymal cells on both sides of the palate. Concurrently, these animals developed severe oral and esophageal adhesions, mirroring the clinical defects observed in humans with *IRF6* mutations [17].

IRF6 has been reported to play a key role in determining the proliferation-differentiation switch of keratinocytes. Mice carrying IRF6 mutations fail to undergo late-stage differentiation, resulting in epidermal hyperplasia. This hyperplasia leads to the formation of multiple epithelial adhesions within the oral cavity, contributing to the development of cleft palate [16]. In the current study, we engineered 293T cells with the newly identified *IRF6* gene mutation. This mutation promoted cell proliferation, consistent with the oral adhesions caused by excessive proliferation of embryonic palate epithelial cells induced by other *IRF6* mutations. Elisabetta Ferretti et al. [18] established a

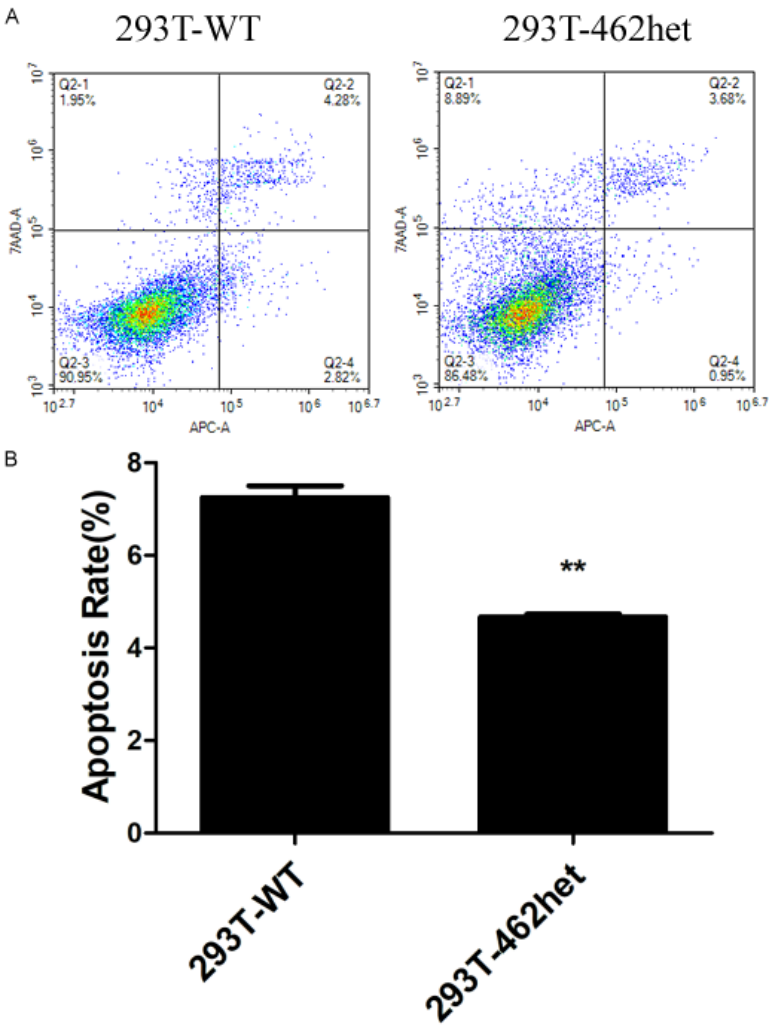

Figure 5. The heterozygous mutation c.1386del (p.A462Pfs*28) within the interferon regulatory transcription factor 6 (*IRF6*) gene inhibited cell apoptosis. A: Apoptosis results. Q2 quadrant cells were positive for 7-aminoactinomycin D staining, representing late apoptosis. Q4 quadrant cells were positive for Annexin V-allophycocyanin staining, representing early apoptosis. B: Comparison of rates of cell apoptosis between groups. The apoptosis rate is the sum of Q2 and Q4. 293T-WT represents wild-type (control) HEK-293T cells, and 293T-462het represents HEK-293T cells heterozygous for the *IFR6* mutation. **P<0.01.

spatiotemporal regulatory module in a mouse model, where Pbx directed midfacial Wnt signaling through the W3 regulatory element. As a result, Wnt effectors activated *p63*, which directly regulates *IRF6*. These findings suggest that an imbalance in the *Wnt-p63-IRF6* regulatory module can lead to localized inhibition of apoptosis at the surface of the facial prominences, contributing to development of cleft lip and palate.

Our experiments also showed that the mutated *IRF6* gene significantly increased cell migration. This migration was associated with downregulation of epithelial cell markers, such as E-cadherin, causing loss of cell adhesion. Concurrently, mesenchymal markers, such as vimentin, were upregulated, enabling cell migration. These findings indicate that *IRF6* gene mutations likely affect key steps of facial fusion by influencing cell migration and EMT. In addition, transforming growth factor beta-3 (TGF-β3) has been reported to promote EMT during palatal fusion by regulating the expression of genes, such as snail family transcriptional repressor 2 (*Snai2)* and *Twist*, in early embryonic palate development [19]. When IRF6 was introduced into TGF-β3-deficient palatal tissue, palate fusion was completed, demonstrating the possible involvement of IRF6 in the TGF-β signaling pathway to regulate genes such as *Snai2* and promote EMT [20].

These observations suggest that *IRF6* mutations may influence different biological processes in cleft lip and palate development via multiple molecular mechanisms. The *IRF6* (c.1386del) variant identified in this study is a *de novo* mutation. A series of functional experiments confirmed that IRF6 may regulate early facial embryogenesis by affecting cell proliferation and migration and promoting EMT. The significant variation in phenotypes in patients with VWS means that some patients may exhibit only minor or irregular depressions in the lips. In such cases, cleft lip and palate surgery may be a viable corrective option. Translational genetics has great potential for aiding in the diagnosis and understanding of

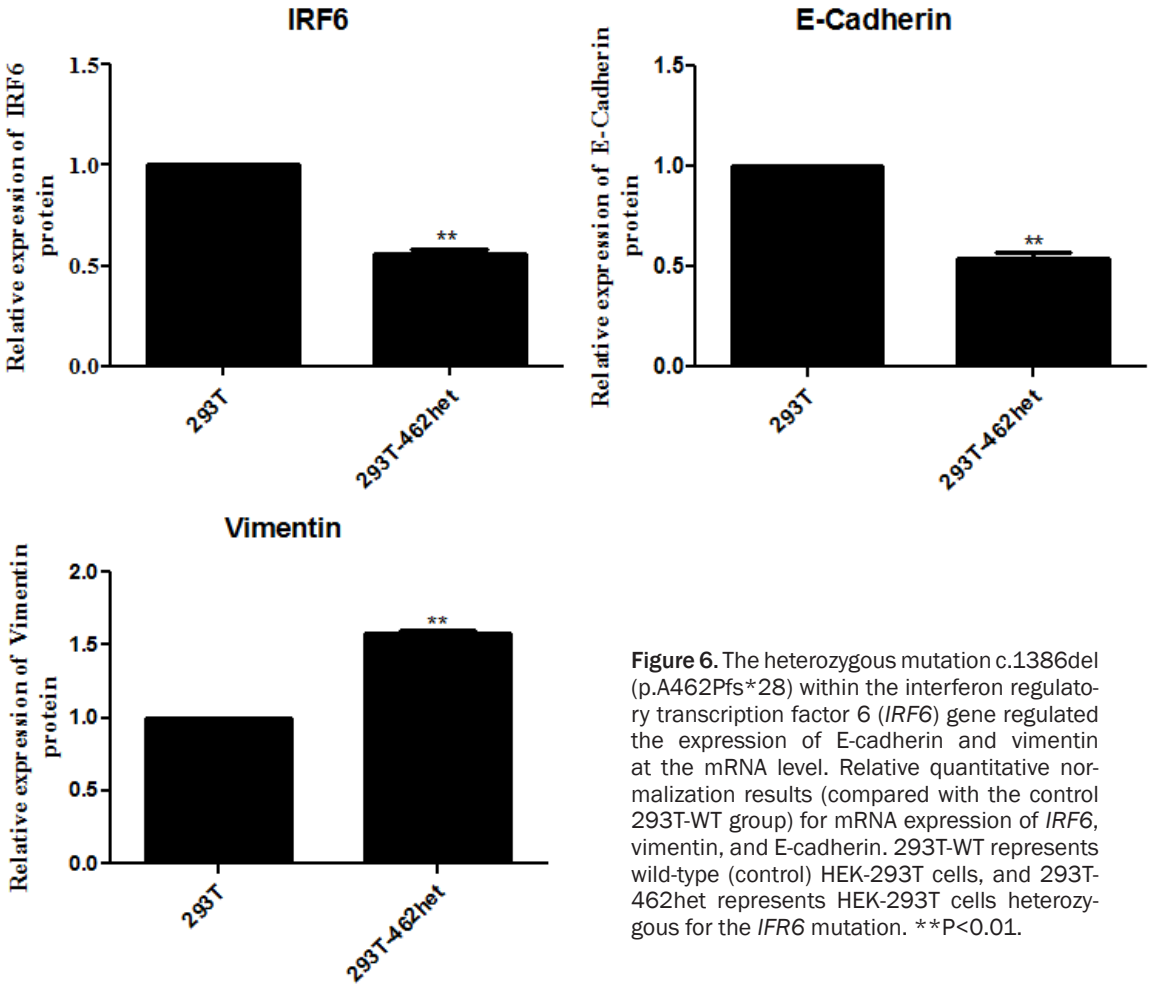

Figure 6. The heterozygous mutation c.1386del (p.A462Pfs*28) within the interferon regulatory transcription factor 6 (*IRF6*) gene regulated the expression of E-cadherin and vimentin at the mRNA level. Relative quantitative normalization results (compared with the control 293T-WT group) for mRNA expression of *IRF6*, vimentin, and E-cadherin. 293T-WT represents wild-type (control) HEK-293T cells, and 293T-462het represents HEK-293T cells heterozygous for the *IFR6* mutation. **P<0.01.

IRF6-related disorders [21]. In clinical practice, diagnosing patients with minor defects and symptoms can be challenging, particularly when comprehensive family data is lacking. Physicians often encounter difficulties in obtaining photographs from all family members to ascertain the type of genetic disease. Consequently, diagnosis may heavily rely on the proband's phenotype and the interrogation of family history. We, therefore, emphasize the importance of evaluating all family members for the presence of lip abnormalities and other VWS-related defects (e.g., dental abnormalities). Although phenotypic variation was present in the family reported in this study, the cause of these differences requires further investigation. We plan to expand the sample size and conduct *in vivo* studies to address this limitation in the future.

Conclusion

In this study, we identified a heterozygous variant c.1386del (p.A462Pfs*28) within the *IRF6* gene in a Chinese pedigree with orofacial clefts inherited in an autosomal dominant manner. This study lays a foundation for future prenatal diagnosis, genetic counseling, and studies of genotype-phenotype relationships. Genetic testing through DNA sequencing is recommended to enable prenatal diagnosis in high-risk pregnancies with a family history of orofacial clefts.

Acknowledgements

The authors would like to thank the patient and her family for their collaboration. The IRF6 gene analysis was conducted in the Department of Prenatal Diagnosis Center (Jinan Maternal and

Child Health Hospital, Jinan), and Yin Feng Gene Technology Co., Ltd. (Jinan). This study was supported by the Key Project of the 2021 National Key Research and Development Program (grant number 2021YFC1005303), Shandong Province Medical and Health Technology Development Plan Project (grant number 202105030122) and Projects of Jinan Science and Technology Bureau (grant numbers 202225064 and 202328017).

The subjects gave written informed consent for the publication of any associated data and accompanying images.

Disclosure of conflict of interest

None.

Address correspondence to: Dr. Hua Jin, Department of Prenatal Diagnosis Center, Jinan Maternal and Child Health Hospital, No. 2 Jianguo Xiaojingsan Road, Shizhong District, Jinan 250001, Shandong, China. E-mail: prenatal123@163.com

References

[1] Reynolds K, Kumari P, Sepulveda Rincon L, Gu R, Ji Y, Kumar S and Zhou CJ. Wnt signaling in orofacial clefts: crosstalk, pathogenesis and models. Dis Model Mech 2019; 12: dmm037051.

[2] Chen L, Yang T, Zheng Z, Yu H, Wang H and Qin J. Birth prevalence of congenital malformations in singleton pregnancies resulting from in vitro fertilization/intracytoplasmic sperm injection worldwide: a systematic review and meta-analysis. Arch Gynecol Obstet 2018; 297: 1115-1130.

[3] Wang M, Yuan Y, Wang Z, Liu D, Wang Z, Sun F, Wang P, Zhu H, Li J, Wu T and Beaty TH. Prevalence of orofacial clefts among live births in China: a systematic review and metairtalysis. Birth Defects Res 2017; 109: 1011-1019.

[4] Mossey PA, Little J, Munger RG, Dixon MJ and Shaw WC. Cleft lip and palate. Lancet 2009; 374: 1773-1785.

[5] Sischo L, Wilson-Genderson M and Broder HL. Quality-of-Life in children with orofacial clefts and caregiver well-being. J Dent Res 2017; 96: 1474-1481.

[6] Wang Z, Lin J, Qiao K, Cai S, Zhang VW, Zhao C and Lu J. Novel mutations in HINT1 gene cause the autosomal recessive axonal neuropathy with neuromyotonia. Eur J Med Genet 2019; 62: 190-194.

[7] Richards S, Aziz N, Bale S, Bick D, Das S, Gastier-Foster J, Grody WW, Hegde M, Lyon E, Spector E, Voelkerding K and Rehm HL. Standards and guidelines for the interpretation of sequence variants: a joint consensus recommendation of the American college of medical genetics and genomics and the association for molecular pathology. Genet Med 2015; 17: 405-424.

[8] Matsuzawa N, Kondo S, Shimozato K, Nagao T, Nakano M, Tsuda M, Hirano A, Niikawa N and Yoshiura K. Two missense mutations of the IRF6 gene in two Japanese families with popliteal pterygium syndrome. Am J Med Genet A 2010; 152A: 2262-2267.

[9] Birnbaum S, Reutter H, Lauster C, Scheer M, Schmidt G, Saffar M, Martini M, Hemprich A, Henschke H, Kramer FJ and Mangold E. Mutation screening in theIRF6 theIRF6IRF6 theIRF6ninapparently nonsyndromic orofacial clefts and a positive family history suggestive of autosomal-dominant inheritance. Am J Med Genet A 2008; 146A: 787-790.

[10] Neves LT, Dionísio TJ, Garbieri TF, Parisi VA, Oliveira FV, Oliveira TM and Santos CF. Novel rare variations in IRF6 in subjects with non-syndromic cleft lip and palate and dental agenesis. Oral Dis 2018; 25: 223-233.

[11] de Lima RL, Hoper SA, Ghassibe M, Cooper ME, Rorick NK, Kondo S, Katz L, Marazita ML, Compton J, Bale S, Hehr U, Dixon MJ, Daack-Hirsch S, Boute O, Bayet B, Revencu N, Verellen-Dumoulin C, Vikkula M, Richieri-Costa A, Moretti-Ferreira D, Murray JC and Schutte BC. Prevalence and nonrandom distribution of exonic mutations in interferon regulatory factor 6 in 307 families with Van der Woude syndrome and 37 families with popliteal pterygium syndrome. Genet Med 2009; 11: 241-247.

[12] Houweling AC, Gille JJ, Baart JA, van Hagen JM and Lachmeijer AM. Variable phenotypic manifestation of IRF6 mutations in the van der woude syndrome and popliteal pterygium syndrome: implications for genetic counseling. Clin Dysmorphol 2009; 18: 225-227.

[13] Kondo S, Schutte BC, Richardson RJ, Bjork BC, Knight AS, Watanabe Y, Howard E, de Lima RL, Daack-Hirsch S, Sander A, McDonald-McGinn DM, Zackai EH, Lammer EJ, Aylsworth AS, Ardinger HH, Lidral AC, Pober BR, Moreno L, Arcos-Burgos M, Valencia C, Houdayer C, Bahuau M, Moretti-Ferreira D, Richieri-Costa A, Dixon MJ and Murray JC. Mutations in IRF6 cause Van der woude and popliteal pterygium syndromes. Nat Genet 2002; 32: 285-289.

[14] Ji Y, Garland MA, Sun B, Zhang S, Reynolds K, McMahon M, Rajakumar R, Islam MS, Liu Y, Chen Y and Zhou CJ. Cellular and developmen-

tal basis of orofacial clefts. Birth Defects Res 2020; 112: 1558-1587.
[15] Losa M, Risolino M, Li B, Hart J, Quintana L, Grishina I, Yang H, Choi IF, Lewicki P, Khan S, Aho R, Feenstra J, Vincent CT, Brown AMC, Ferretti E, Williams T and Selleri L. Face morphogenesis is promoted by Pbx-dependent EMT via regulation of Snail1 during frontonasal prominence fusion. Development 2018; 145: dev157628.
[16] Richardson RJ, Dixon J, Malhotra S, Hardman MJ, Knowles L, Boot-Handford RP, Shore P, Whitmarsh A and Dixon MJ. Irf6 is a key determinant of the keratinocyte proliferation-differentiation switch. Nat Genet 2006; 38: 1329-1334.
[17] Lin Y, Xu D, Li X, Liu C, Liu X, Huang S, Huang Y and Liu X. Upregulation of interferon regulatory factor 6 promotes neuronal apoptosis after traumatic brain injury in adult rats. Cell Mol Neurobiol 2015; 36: 27-36.
[18] Ferretti E, Li B, Zewdu R, Wells V, Hebert Jean M, Karner C, Anderson Matthew J, Williams T, Dixon J, Dixon Michael J, Depew Michael J and Selleri L. A conserved Pbx-Wnt-p63-Irf6 regulatory module controls face morphogenesis by promoting epithelial apoptosis. Dev Cell 2011; 21: 627-641.
[19] Prasad CP, Rath G, Mathur S, Bhatnagar D, Parshad R and Ralhan R. Expression analysis of E-cadherin, Slug and GSK3β in invasive ductal carcinoma of breast. BMC Cancer 2009; 9: 325.
[20] Ke CY, Xiao WL, Chen CM, Lo LJ and Wong FH. IRF6 is the mediator of TGFβ3 during regulation of the epithelial mesenchymal transition and palatal fusion. Sci Rep 2015; 5: 12791.
[21] Grouse L. Translational genetic research of complex diseases. J Transl Intern Med 2015; 3: 137-143.